$$K(z,+) = K(z,-) = K \quad ,$$

where K is defined in (1) and (2). Careful experiments show, however, that $K(z,+)$ and $K(z,-)$ are generally distinct numbers that do change with depth. Furthermore, we shall see in Sec. 10.7 that, in homogeneous media,

$$\lim_{z\to\infty} K(z,+) = \lim_{z\to\infty} K(z,-) = k_\infty$$

where k_∞ is a number which depends only on the inherent optical properties of the medium and is completely independent of the external lighting conditions on the upper boundary of the medium. One of the goals of the present chapter is to find out something about the nonlinear behavior of $K(z,\pm)$ at relatively *small* depths.

The quantity $R(z,-)$ summarizes the flux transmitting and reflecting properties of the medium both above and below the hypothetical plane at depth z. According to the simple formulas (1) and (2),

$$R(z,-) = \frac{H(0,+)}{H(0,-)} \quad ,$$

a fixed number for all z. Careful experiments show, however, that $R(z,-)$ changes with depth; and in all homogeneous media it will be shown (Sec. 10.7), to approach a well-defined limit as $z\to\infty$:

$$\lim_{z\to\infty} R(z,-) = R_\infty \quad ,$$

where R_∞ is a number which depends only on the inherent optical properties of the hydrosol and is completely independent of the external lighting conditions on the upper boundary of the medium. Another of our present goals is to understand the nonlinear behavior of $R(z,-)$ for relatively small values of z.

10.2 Experimental Basis for the Shallow Depth Theory

To prepare the groundwork leading to the theory of the light field at shallow depths, we now consider some experimental data which supplies graphic evidence of the nonlinear depth behavior of $K(z,\pm)$ and $R(z,-)$ in near-surface regions of a specific hydrosol. The experimental evidence presented in this and the following sections has been computed from the data obtained in Lake Pend Oreille, Idaho, by J. E. Tyler [298].

Figure 10.1 depicts the semilog plots of $H(z,+)$ and $H(z,-)$ over the range of depths $5 \le z \le 55$ meters; $H(z,\pm)$ are associated with a wavelength interval of width 64 mμ centered at 480 mμ. This depth range corresponds to a range of about 20 optical depths, so that the light field in the vicinity of 50 meters should have for all practical purposes attained the asymptotic limit--assuming complete homogeneity of the medium.

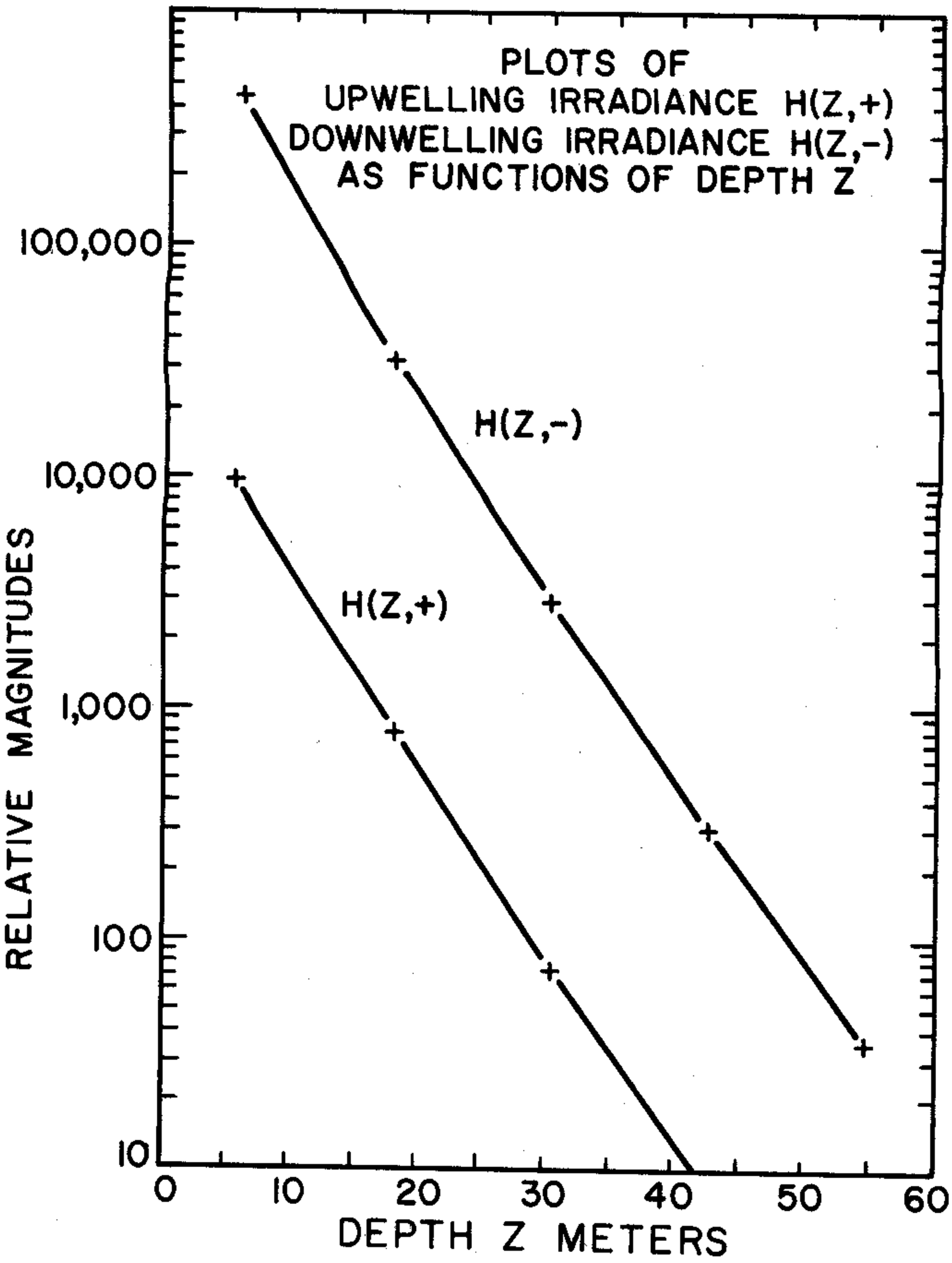

FIG. 10.1 Irradiance plots (480 mμ) from Tyler's study of Lake Pend Oreille, Idaho, spring 1957.

Just how close is the present hydrosol to being homogeneous? To answer this, we must know the values of the volume attenuation function α within the medium. Figure 10.2 shows a plot of α versus depth for the present medium. An optical medium is by definition *homogeneous* if α is a constant function within that medium. It is clear from the α plot of Figure 10.2 that the hydrosol was not strictly homogeneous at the time of the experiment. There is about a 12 percent variation in the values of α over the indicated depth range. In several places, in particular the bracketed range, there is a relatively abrupt change of the order of 5 percent in the values of α. For many practical purposes these changes are negligible. However, for the specific purposes of the present discussion, these changes are of extreme interest. In addition to $\alpha(z)$, the values $a(z)$ of the volume absorption function are plotted for several depths.

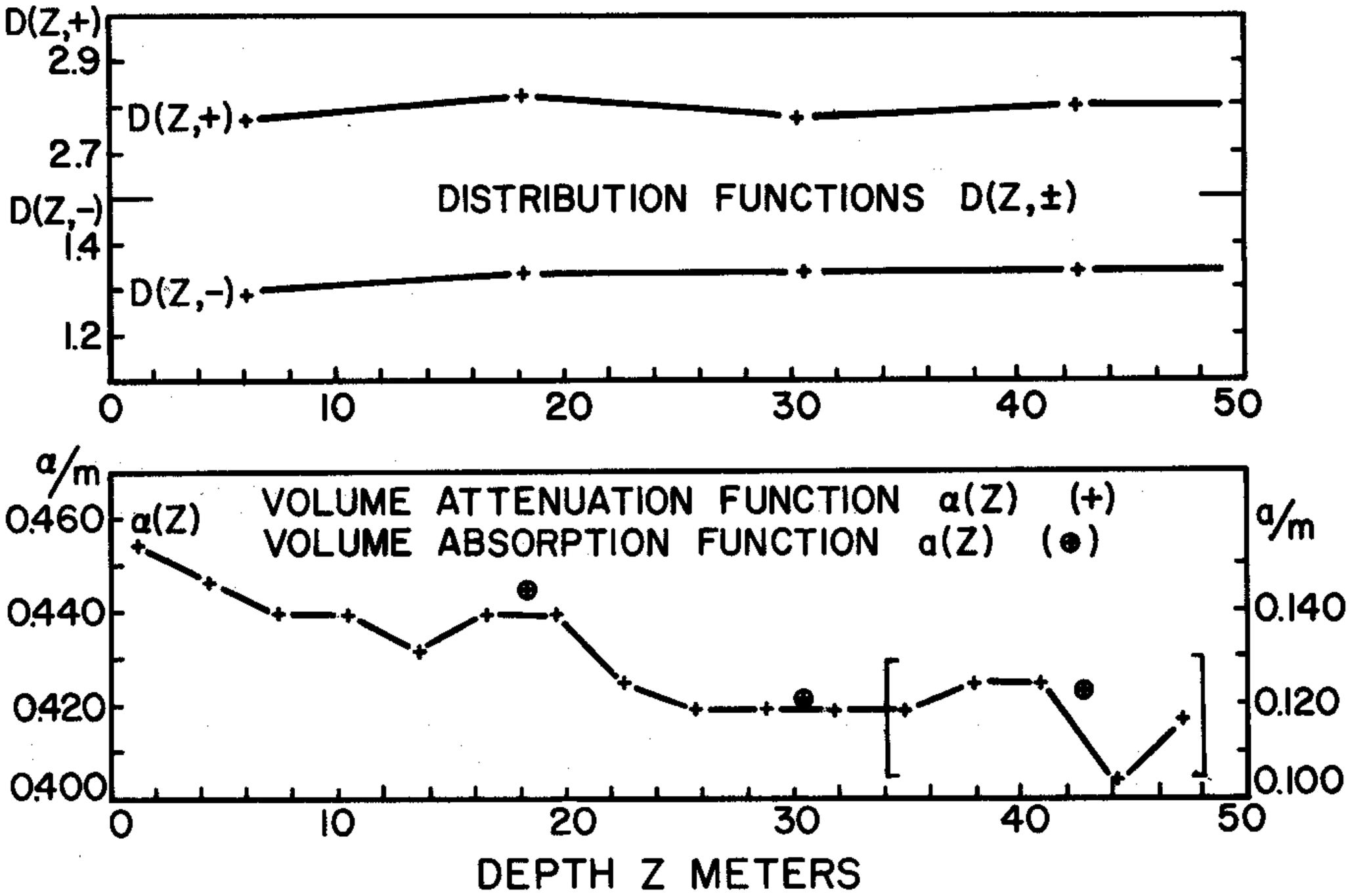

FIG. 10.2 Optical properties $\alpha(z)$, $a(z)$, and $D(z,\pm)$ of Lake Pend Oreille, Idaho (for 480 mμ) as determined by Tyler in spring 1975.

Observe how the values $a(z)$ tend to follow the changes in $\alpha(z)$. This feature will be noted again later in this study when the mathematical model is being discussed. With this background information in mind we may now turn to a detailed examination of the plots of $H(z,\pm)$.

Observe that each of the plots in Fig. 10.1 exhibits a small but noticeable nonlinearity. The curves are slightly concave upward, indicating relatively steep slope at shallow depths and less steep slopes at greater depths. To facilitate the examination of the logarithmic slopes, they have been plotted as functions of depth in Fig. 10.3. Both $K(z,+)$ and $K(z,-)$ exhibit a uniform downward trend toward a common asymptote defined by the horizontal line across the figure at ordinate $k_\infty = 0.178$/meter. This value was obtained using the fact, cited earlier, that $K(z,\pm)$ has a common limit and then performing a suitable extrapolation based on this fact (see Ref. [263]).

The uniform approach of $K(z,\pm)$ to this common limit appears to be interrupted in the neighborhood of 40 meters. There appears to be some optical disturbance in the medium within the immediate depth range (bracketed in Fig. 10.3) that results in a marked deviation of these curves from their expected paths. We can explain this anomalous behavior on the basis of our observations of the depth dependence of $\alpha(z)$ in Fig. 10.2. The abrupt change in the values of α in the same depth range appear to hold the key to the explanation when the following formulas are examined:

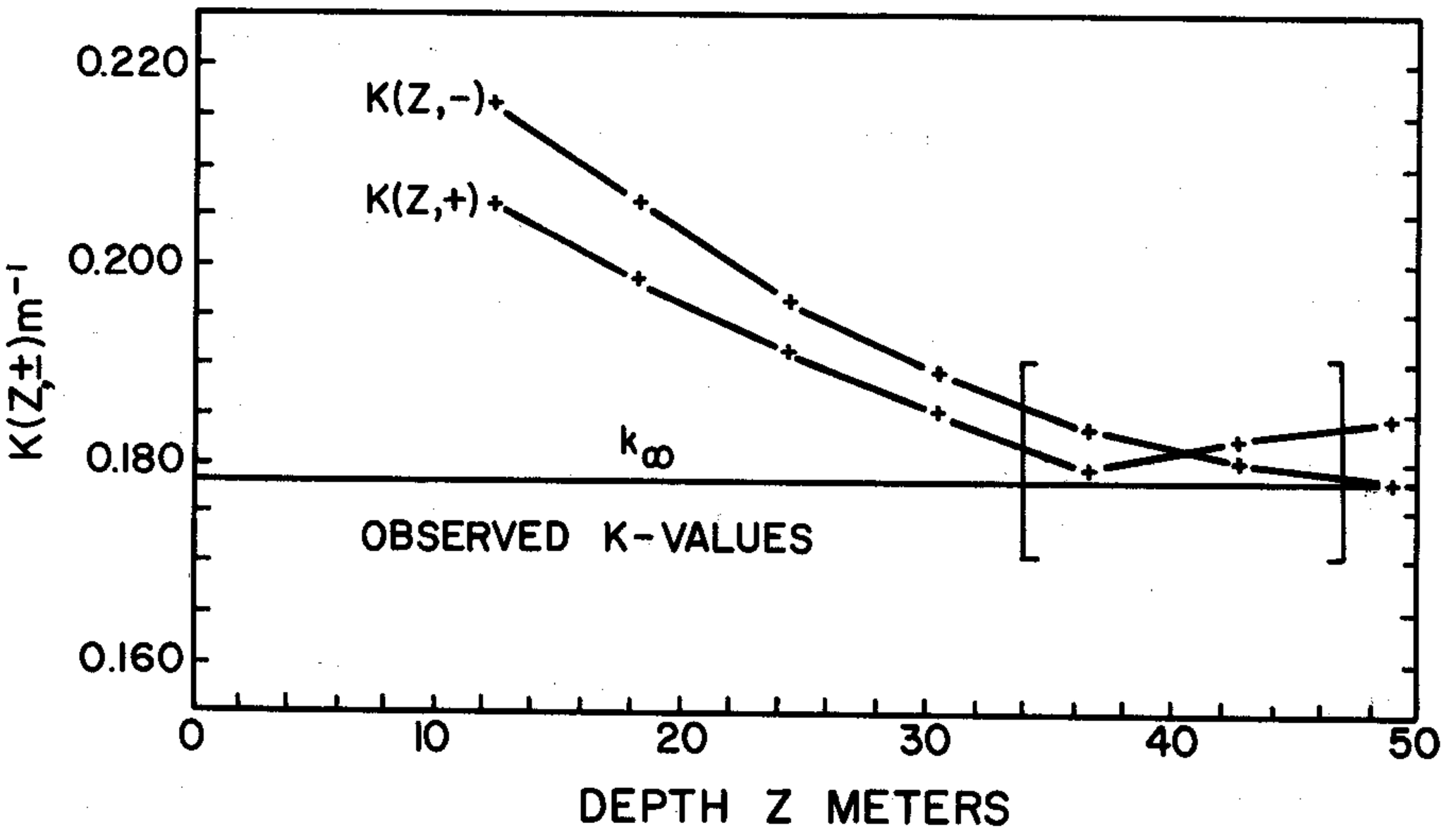

FIG. 10.3 K-function values (at 480 mμ) for Lake Pend Oreille, Idaho, spring 1957, computed from Tyler's data.

$$K(z,-) = \alpha(z,-) - \frac{\int_{\Xi_-} N_*(z,\xi)\, d\Omega(\xi)}{H(z,-)} \quad , \qquad (1)$$

$$K(z,+) = -\alpha(z,+) + \frac{\int_{\Xi_+} N_*(z,\xi)\, d\Omega(\xi)}{H(z,+)} \quad . \qquad (2)$$

These are exact formulas relating $K(z,\pm)$ to the values of α and the angular distribution of the light field at depth z. These formulas need not be derived here; they readily follow from the representations of the K-functions in (18) and (19) of Sec. 9.2. See the derivation of (26) of Sec. 9.2. Moreover, the definitions of the quantities $\alpha(z,\pm)$:

$$\alpha(z,\pm) = \alpha(z)D(z,\pm)$$

are given in Sec. 8.3. Here $D(z,\pm)$ are the values of the *distribution functions for the downwelling (-) and upwelling* (+) streams of radiant flux at depth z. Figure 10.2 shows a plot of $D(z,+)$ and $D(z,-)$ for the present hydrosol. It is evident that these quantities are nearly constant over the entire depth range under study.

On the basis of (1), whenever there is an abrupt change in the values $\alpha(z)$ over some small depth interval and whenever $D(z,-)$ is relatively fixed over this depth interval (so that the integral term is relatively constant), we predict that $K(z,-)$ must exhibit a change in the *same direction* as that of $\alpha(z)$. Thus if $\alpha(z)$ abruptly decreases, $K(z,-)$ is expected to exhibit a decrease in value.

On the basis of (2), on the other hand, under the same conditions, we should expect a simultaneous change of $K(z,+)$, but in the *opposite direction* as that of $\alpha(z)$. Thus if $\alpha(z)$ abruptly decreases, $K(z,+)$ is expected to exhibit an increase in value.

Returning now to Figs. 10.3 and 10.2, these predictions are apparently borne out by the portions of the α, and K curves in the bracketed depth range. Therefore the abrupt inhomogeneity in the structure of the hydrosol in this depth range appears to induce the observed interruption of the orderly trend of the K-curves toward their limit.

One might inquire why the comparable change in α in the vicinity of 20 meters does not produce a similar marked effect on the K-curves. The answer lies in the fact that the light field in the vicinity of 5-30 meters (2-12 attenuation lengths) is evidently still in the process of settling down and attaining a spatial steady state configuration, so that changes in K-values are naturally relatively great in this region; changes in α-values thus have relatively little additional influence on the fine structure of the K-functions, and their effects are obscured by the settling-down changes taking place. However, at around 40 meters (about 16 attenuation lengths) the light field has begun to assume its asymptotic angular structure. Any abrupt change in $\alpha(z)$ would now cause the entire smoothing process to recommence; in particular the K-values are now very close to their limit, and the effect of any inhomogeneity would be relatively magnified.

As a final step in the examination of the experimental evidence, we turn to Fig. 10.4 which exhibits a plot of $R(z,-)$ versus depth. In this case there is a uniform upward trend, as depth increases, of the values of $R(z,-)$ toward the limiting value $R_\infty = 0.0278$. This limiting value may be found from the formula:

$$R_\infty = \frac{k_\infty - a(-)}{k_\infty + a(+)} \qquad (3)$$

where

$$a(\pm) = aD(\pm) \quad .$$

The quantities $D(\pm)$ are the limits of $D(z,\pm)$ as $z \to \infty$, and are found from the plots of $D(z,\pm)$ in Fig. 10.2. The values used were $D(+) = 2.77$, $D(-) = 1.33$; k_∞ is as defined in Fig. 10.3 and a was taken as the value of the volume absorption function at depth 42 meters: $a(42) = 0.123$ per meter. The basis for (3) will be established in Sec. 10.7. However,

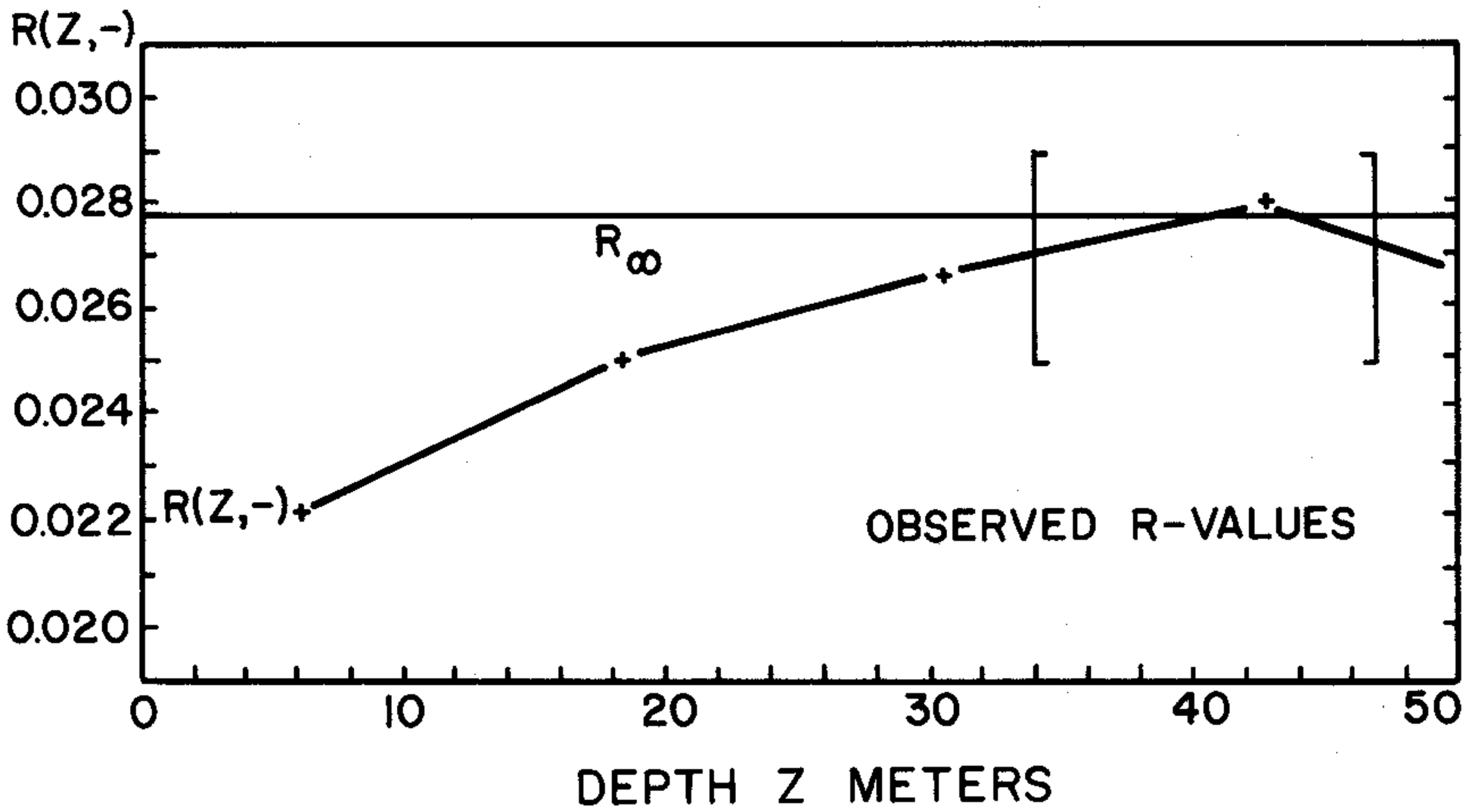

FIG. 10.4 Reflectance function data (at 480 mμ) for Lake Pend Oreille, Idaho, spring 1957, computed from Tyler's data.

we already have a version of it given us by the two-D model for irradiances in (102) of Sec. 8.7.

As in the case of the plots of $K(z,\pm)$, the plot of $R(z,-)$ exhibits a change in trend in the bracketed depth range discussed earlier. From the exact representation:

$$R(z,-) = \frac{K(z,-) - a(z,-)}{K(z,+) + a(z,+)}$$

of the function $R(z,-)$ (given in (25) of Sec. 9.2), and the observed changes in $K(z,+)$ and $K(z,-)$, we see that the observed anomaly, namely the downward trend exhibited by $R(z,-)$ in the vicinity of 40 meters, is traceable directly to the abrupt change of $\alpha(z)$ in this vicinity. Another way to see the cause of the change of slope of $R(z,-)$ in Fig. 10.4 is to examine (32) of Sec. 9.2 in the neighborhood of the crossing of the K-curves in Fig. 10.3.

Summary of the Experimental Evidence

We may now summarize the preceding observations:

(a) Over the depth ranges where the hydrosol is practically homogeneous, the magnitudes of the K-functions exhibit a *monotonic* decrease with increasing depth, with $K(z,-) > K(z,+)$. It appears that if the medium were homogeneous and infinitely optically deep. the monotonic decrease would continue indefinitely toward a common limit k_∞.

(b) Under the same conditions as in (a), the values $R(z,-)$ appear to exhibit a *monotonic* increase toward a well-defined limit R_∞.

(c) The distribution functions $D(z,\pm)$ are *practically constant* with depth.

(d) The ratio of $\alpha(z)$ to $a(z)$ and hence the ratio $s(z)/\alpha(z)$, where $\alpha(z) = a(z) + s(z)$, appears to be *practically constant* with depth.

<< Table of Contents **<< Title Page >>** **Next Page >>**

10.3 Formulation of the Shallow-Depth Model for K and R Functions

On the basis of the experimental evidence summarized in Sec. 10.2, in particular statements (c) and (d), we may adopt the two-D model of the light field as developed in Sec. 8.5. The equations forming the basis of this model have been explored in detail throughout Chapter 8. Therefore it simply remains to solve the equations of this model for the particular context at hand. We shall adopt the two-D model for decomposed light fields as given in Sec. 8.5. In addition to the assumptions leading to (67) of Sec. 8.5, we specifically emphasize that the optical medium is:

(i) Optically infinite deep.

(ii) Separable. (The ratio of $s(z)/\alpha(z)$ is invariant with depth--see experimental statement (d) of Sec. 10.2.)

(iii) Irradiated by a collimated radiance distribution of magnitude N° incident at an angle θ_o from the normal to its upper boundary.

Formulas for $H(z,\pm)$

It follows from the two-D theory, in particular (71)-(73) of Sec. 8.5, that under the present conditions the expressions for $H(z,\pm)$ $(= H^\circ(z,\pm) + H^*(z,\pm))$ are:

$$H(z,-) = N^\circ \left[C(\mu_o,-)e^{-k_\infty z} + [\mu_o - C(\mu_o,-) \cdot e^{-\alpha z/\mu_o} \right] \quad (1)$$

$$H(z,+) = N^\circ \left[C(\mu_o,-)R_\infty e^{-k_\infty z} - C(\mu_o,+)e^{-\alpha z/\mu_o} \right] \quad (2)$$

The quantities $C(\mu_o,\pm)$, k_∞, and R_∞ and their component parts are defined in detail in Sec. 8.5. It is of interest to compare (1) and (2) with (37) and (38) of Sec. 8.6. For convenience we repeat basic formulas of Sec. 8.5; (72) of Sec. 8.5 is of the form:

$$C(\mu_o,\pm) = \frac{\sigma_\pm(\mu_o)b^*(\mp) + \sigma_\pm(\mu_o)\left[a^*(\mp) + b^*(\mp) \mp \left(\frac{\alpha}{\mu_o}\right)\right]}{\left(k_+ + \frac{\alpha}{\mu_o}\right)\left(k_- + \frac{\alpha}{\mu_o}\right)} \quad (3)$$

where $\mu_o = \cos\theta_o$ (cf. (70) of Sec. 8.5). Furthermore: